Supplemental Material for 'Electric and Magnetic Tuning Between the Trivial and Topological Phases in InAs/GaSb Double Quantum Wells'

Fanming Qu[1,*], Arjan J. A. Beukman[1,*], Stevan Nadj-Perge[1], Michael Wimmer[1], Binh-Minh Nguyen[2], Wei Yi[2], Jacob Thorp[2], Marko Sokolich[2], Andrey A. Kiselev[2], Michael J. Manfra[3], Charles M. Marcus[4], Leo P. Kouwenhoven[1,§]

[1] QuTech and Kavli Institute of Nanoscience, Delft University of Technology, 2600 GA Delft, The Netherlands

[2] HRL Laboratories, 3011 Malibu Canyon Rd, Malibu, CA 90265, USA

[3] Department of Physics, Purdue University, West Lafayette, Indiana 47907, USA

[4] Center for Quantum Devices, Niels Bohr Institute, University of Copenhagen, 2100 Copenhagen, Denmark

[*] These authors contributed equally to this work.

[§] l.p.kouwenhoven@tudelft.nl

I. Two-carrier model

When electron and hole gases coexist in a two-dimensional system, the dependence of Hall resistance R_{xy} on perpendicular magnetic field B is [1]:

$$R_{xy} = \frac{-B[(n\mu_e{}^2 - p\mu_h{}^2) + B^2\mu_e{}^2\mu_h{}^2(n-p)]}{e[(n\mu_e + p\mu_h)^2 + B^2\mu_e{}^2\mu_h{}^2(n-p)^2]}$$

where n and p are the densities for electrons and holes, respectively; μ_e and μ_h are the corresponding mobilities. The measured Hall trace can be fitted using the formula above, and a constraint is given by the zero-field longitudinal resistance:

$$B = 0: \quad R_{xx} = \frac{L}{e(n\mu_e + p\mu_h)W}$$

where L and W are the length and width of the Hall bar, respectively.

In the limit of $B \gg 1/\mu_e$, $1/\mu_h$, $R_{xy} \approx \frac{B}{(p-n)e}$.

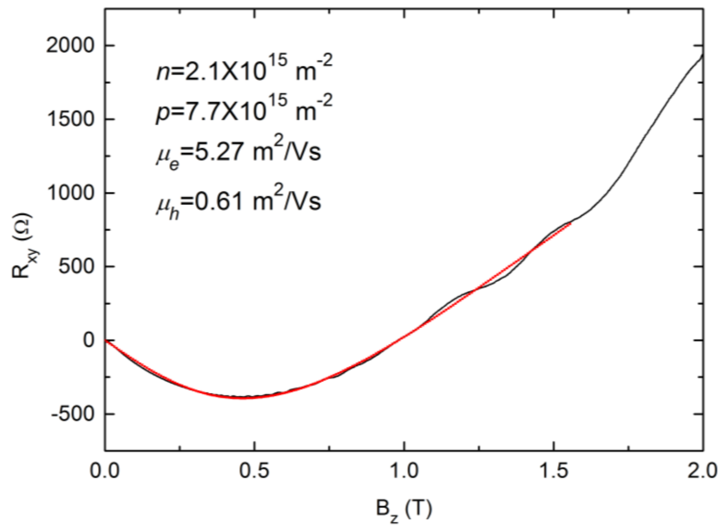

Figure S1: An example of two-carrier model fitting (red) of the Hall trace (black) taken at position 1 on line L in Fig. 2(a) in the main text. The zero-field longitudinal resistance is used as the constraint. The extracted carrier densities and mobilities are shown in the figure.

II. Dingle plot

For a two-dimensional electron gas in a perpendicular magnetic field B, the amplitude of the Shubnikov-de Haas (SdH) oscillations, ΔR, is given by:

$$\Delta R = 4R_0 \exp\left(\frac{-\pi m_e}{eB\tau_q}\right)\frac{2\pi^2 m_e k_B T}{e\hbar B} / \sinh\left(\frac{2\pi^2 m_e k_B T}{e\hbar B}\right)$$

where R_0 is the zero-field resistance, m_e the effective electron mass, and τ_q the quantum scattering time. At a fixed magnetic field B, by measuring the temperature dependence of ΔR, m_e and τ_q can be extracted from the fit, the so called Dingle plot.

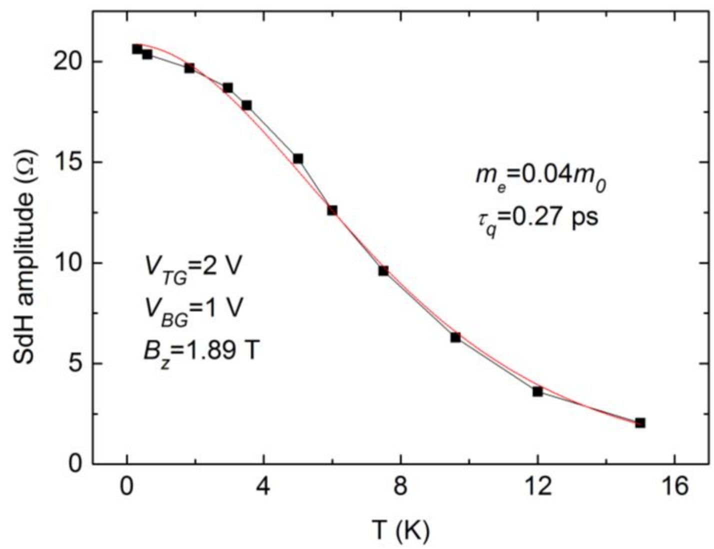

Figure S2: Dingle plot taken deep in the electron regime, where V_{TG}=2 V and V_{BG}=1 V for device #1 in the main text. The fit (red) of the temperature dependence of the SdH oscillation amplitude (black) gives the effective electron mass m_e=0.04m_0 (m_0 is the electron mass), and the quantum scattering time τ_q=0.27 ps. (Deep in the hole regime, the Dingle plot gives the effective hole mass m_h=0.09m_0.)

III. Calculation of the phase diagram

A simple capacitor model (Fig. S3) is used to simulate the phase diagram of the InAs/GaSb double quantum wells (DQWs). The result (Fig. S4) is in qualitative agreement with the calculations by Liu et al. [2].

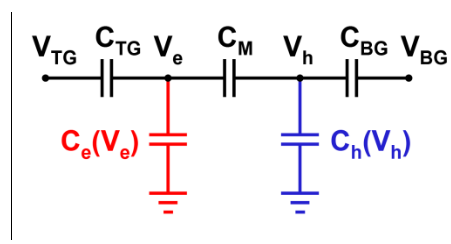

Figure S3: Capacitor model of the InAs/GaSb double quantum wells device.

The device operation can be explored and semi-quantitatively understood by considering electrostatics of its stack in the simplistic *equivalent capacitance model* [3] which is shown in Fig. S3. Here C_{TG}, C_M, and C_{BG} are *geometric* capacitances between the top gate and the two-dimensional electron gas (2DEG) (or, more accurately, 2DEG electron density center plane located inside the InAs layer), between 2DEG and two-dimensional hole gas (2DHG), and between 2DHG and the back gate, respectively. C_e and C_h are *quantum* capacitances reflecting an energy penalty associated with the gradual filling of electron/hole states. It is proportional to the density of states D. For a 2D subband in a parabolic approximation, $D = |m| / \pi\hbar^2$ is a constant defined by the subband in-plane effective mass m. The penalty is zero when the corresponding subband is fully depleted, as D=0 in this case. With the Fermi surfaces of electron and hole 2D gases grounded through the Ohmic contacts, electron and hole accumulation can be parameterized by the energies of the electron and hole subband extrema, $-|e|V_e$ and $-|e|V_h$. Thus, $C_{e,h}$ are *piecewise constant* functions of $V_{e,h}$: $C_e=e^2D_e$ when $V_e>0$ (and is zero otherwise), while $C_h=e^2D_h$ only when $V_h<0$. This model can be numerically solved for $V_{e,h}$ at arbitrary back and top gate biases (V_{BG},V_{TG}), to obtain the electron ($n=C_eV_e/|e|$) and hole ($p=-C_hV_h/|e|$) densities.

This simplistic model reproduces the anticipated physics well, resolving conditions in gate space when a normal gap forms (i.e., no conduction: $n=p=0$), single carrier situations (either n=0 or p=0), and when both electrons and holes are present simultaneously. The resulting phase diagram is shown in Fig. S4. It marks electron and hole depletion boundaries $V_{e,h}$=0 (green lines), charge neutrality line $n=p$ (dashed), and a zero-gap condition $V_e=V_h$ (yellow line). Constant density contours for both electrons and holes are also shown. Geometric capacitances $C_{TG}=3.6\text{x}10^{11}|e|V^{-1}cm^{-2}$ =58 nF cm^{-2}, $C_M=9.8\text{x}10^{12}|e|V^{-1}cm^{-2}$ =1.6 uF cm^{-2}, and $C_{BG}=4.9\text{x}10^{11}|e|V^{-1}cm^{-2}$ =79 nFcm^{-2} have been estimated for the actual multilayer dielectric/semiconductor stack using $\varepsilon_{\rm SiN}=7.0$, $\varepsilon_{\rm GaSb}=15.7$, $\varepsilon_{\rm AlSb}=10.9$, and $\varepsilon_{\rm InAs}=15.5$ dielectric constants, assuming that electron and hole central planes coincide with centers of InAs and GaSb layers, and that V_{BG} is applied to the edge of the n-doped GaSb substrate. Experimentally determined $m_e=0.04m_0$ and $m_h=0.09m_0$ have been used to set quantum capacitance values at $C_e=1.7\text{x}10^{13}|e|V^{-1}cm^{-2}$ =2.7 uFcm^{-2} and $C_h=3.8\text{x}10^{13}\,|e|V^{-1}cm^{-2}$ =6.0 uFcm^{-2}.

The above simple model does not include $C_{e,h}$ modulation due to electron and (especially) hole non-parabolicities, the spatial shift of the wave functions inside the InAs and GaSb layers, as well as other details related to the band alignment in the device.

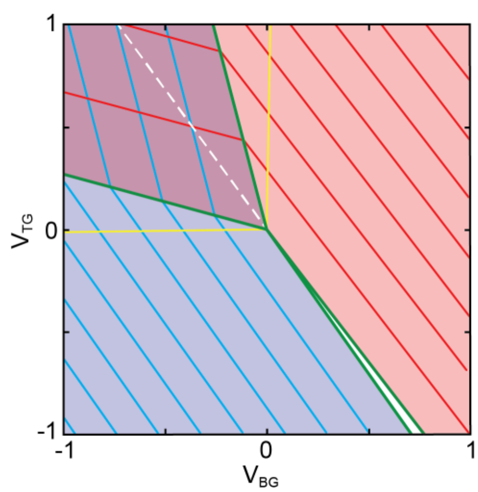

Figure S4: Simulation result from the capacitor model. Red and blue shaded areas indicate regions of purely electrons and holes, respectively. The purple shaded area indicates a region where electrons and holes coexist. Red and blue lines represent equal density of electrons and holes, respectively. The yellow lines indicate points where the two bands touch each other. The white region at the bottom right part of the figure indicates the normal insulating gap. The dotted white line at the top left part connect points where electrons and holes have equal density and the hybridization gap is expected.

IV. Supplementary Figures

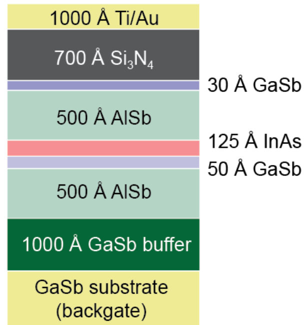

Figure S5: Cross-section of the InAs/GaSb DQWs used in the main text. The quantum well contains a 12.5 nm InAs layer on top of a 5 nm GaSb layer. The structure is grown on a doped GaSb substrate.

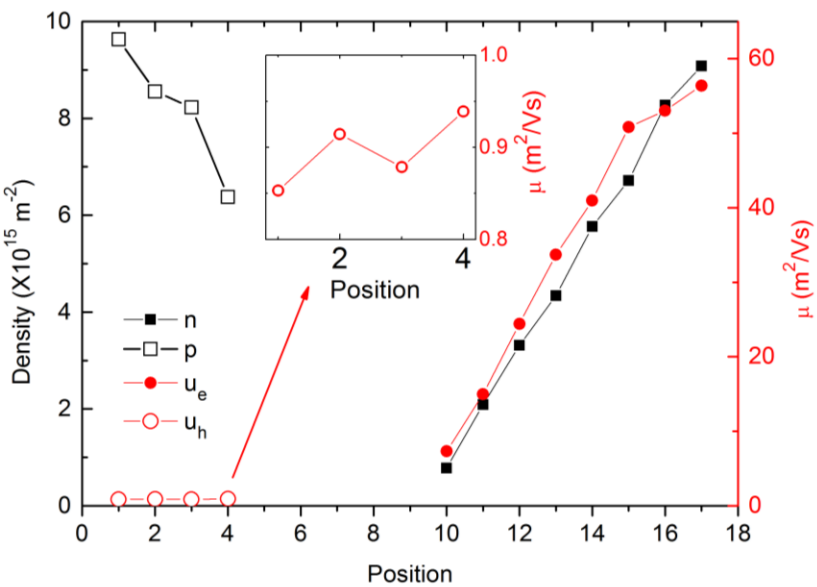

Figure S6: Densities and mobilities for electrons and holes for device #1 along line R in Fig. 2(a) in the main text. The electron mobility is more than one order of magnitude higher than the hole mobility. Because of the application of the GaSb substrate, record values of the electron mobility are achieved.

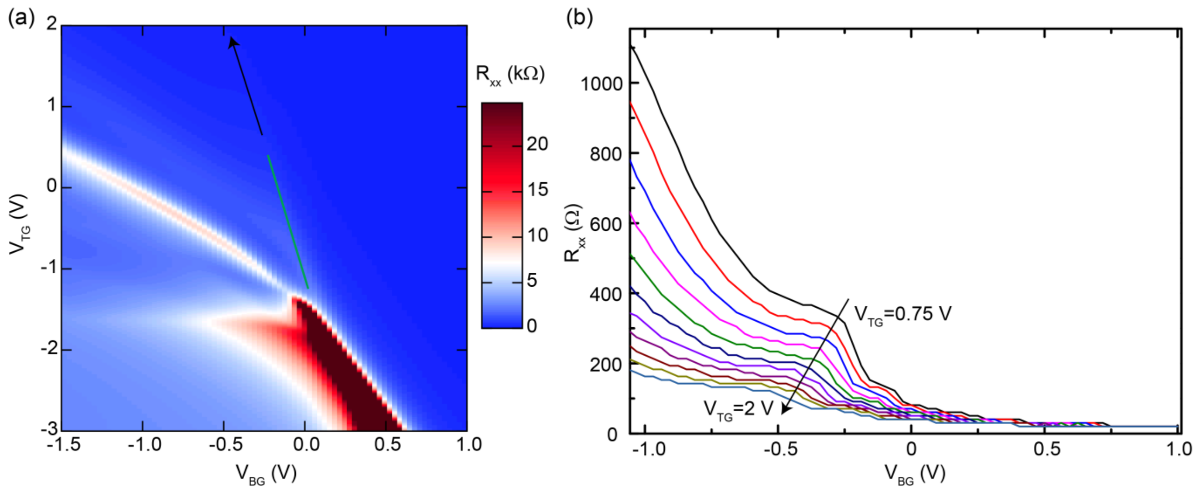

Figure S7: (a) Longitudinal resistance as a function of back gate and top gate voltages for device #2 in the main text measured at 300 mK, which shows nominally the same phase diagram as Fig. 2(a) for device #1 in the main text. The green line indicates the onset of the coexistence of electrons and holes. (b) Line cuts taken from (a) between V_{TG}=0.75 V and 2 V. The arrow shows the shift of the small resistance peak, consistent with the arrow in (a).

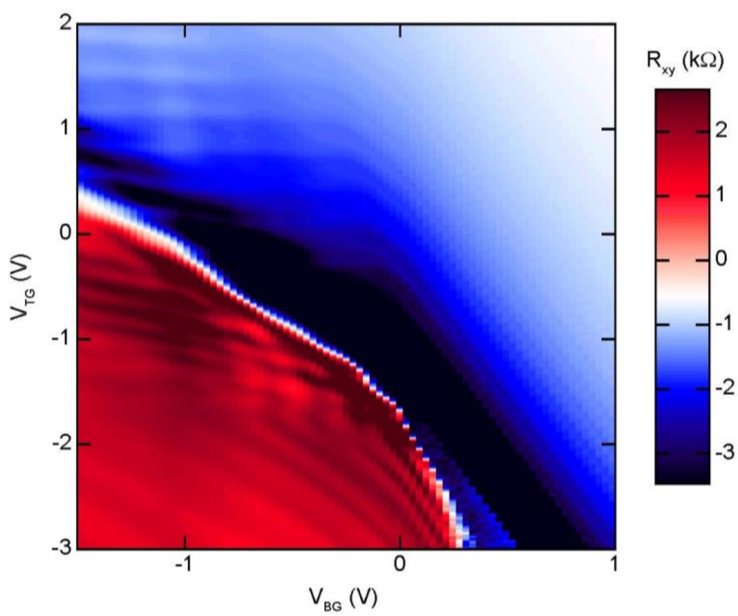

Figure S8: Hall resistance as a function of both top gate and back gate voltages at a fixed perpendicular magnetic field of 2 T for device #1 in the main text. This figure was measured simultaneously with Fig. 4 in the main text. For regions with only holes or a majority of holes, the Hall resistance shows positive values, as shown by the red color. In contrast, the blue color indicates regions with only electrons or a majority of electrons.

V. Size of the hybridization gap

To give a rough estimate on the size of the hybridization gap, we take gate positions 6 and 10 in Fig. 2(a) in the main text as the gap edges. Combining the electron density difference between the two selected points based on a linear extrapolation of n_{SdH} and the constant 2D density of states $m_e/\pi\hbar^2$, we estimate a gap size of $\Delta = \pi\hbar^2(n_{10} - n_6)/m_e$=9.3 meV, which is larger than values reported in the literature. The effective mass of m_e=0.04m_0 for electrons is deduced from the temperature dependence of the amplitude of SdH oscillations, i.e., the Dingle plot, deep in the electron regime (V_{BG}=1 V, V_{TG}=2 V) where n=2.2×10^{16} m^{-2} and μ_e=70 m^2/Vs. The relatively large deduced gap may be overestimated due to the inaccuracy of the selected gap edge positions, or it is indeed large because of strong coupling between electrons and holes for these gate values. We also notice that at the upper-left side of gapped region I (larger k_{cross}) in Fig. 2(a) the peak resistance drops, indicating a decrease of the hybridization gap. Such decrease is presumably due to a reduced wave function overlap and hence a reduced coupling strength, in spite of the increased k_{cross}. From the Dingle plot deep in the electron regime we extract a quantum scattering time of τ_q=0.27 ps, corresponding to a quantum level broadening of $\Gamma_e = \hbar/2\tau_q$=1.22 meV. However, close to the gap, the electron mobility drops by more than one order of amplitude (μ_e=5.5 m^2/Vs at position 5), suggesting a much larger Γ_e. Hence, the total level broadening will be $\Gamma = \Gamma_e + \Gamma_h \gg 1.22$ meV (where Γ_h represents the hole contribution), which could account for the relatively low resistance at the hybridization gap.

References:

[1] R. Smith, *Semiconductors* (Cambridge University Press, Cambridge, 1978).

[2] C. X. Liu *et al.*, Phys. Rev. Lett. **100**, 236601 (2008).

[3] S. Luryi, Appl. Phys. Lett. **52**, 501 (1988).